

Aggregation Dynamics of Active Rotating Particles in Dense Passive Media

Juan L. Aragonés,* Joshua P. Steimel,* and Alfredo Alexander-Katz†

*Department of Materials Science and Engineering,
Massachusetts Institute of Technology,
Cambridge, MA, 02139, USA.*

(Dated: December 13, 2021)

Active matter systems are able to exhibit emergent non-equilibrium states due to activity-induced effective interactions between the active particles. Here we study the aggregation and dynamical behavior of active rotating particles, spinners, embedded in 2D passive colloidal monolayers, which constitutes one such non-equilibrium process. Using both experiments and simulations we observe aggregation of active particles or spinners whose behavior resembles classical 2D coarsening. The aggregation behavior and spinner attraction depends on the mechanical properties of the passive monolayer and the activity of spinners. Spinner aggregation only occurs when the passive monolayer behaves elastically and when the spinner activity exceeds a minimum activity threshold. Interestingly for the spinner concentrations investigated here, the spinner concentration doesn't seem to change the dynamics of the aggregation behavior. There is also a characteristic cluster size at which the dynamics of spinner aggregation is maximized as drag through the passive monolayer is minimized and the stress applied on the passive medium is maximized. We also show that a ternary mixture of passive particles, co-rotating, and counter-rotating spinners also aggregates into clusters of co and counter-rotating spinners respectively.

I. INTRODUCTION

Attractive interactions between particles in a homogeneous mixture induces the formation of clusters. These clusters grow in time until the mixture separates into two distinct phases. The dynamics of phase separation in binary mixtures is fairly well characterized [1]; and depends on the dimensionality, thermodynamic conditions, and type of cluster growth. Often, these attractive interactions are induced by direct chemical interactions. Alternatively, they can also be induced by electromagnetic, phoretic [2], collisions [3] or hydrodynamic forces [4–6]. Non-equilibrium interactions can also promote particle aggregation. Because of the out-of-equilibrium nature of active matter systems, these are excellent candidates to study novel mechanisms of particle aggregation and subsequent phase separation.

Active matter systems are composed of active agents that consume energy from their environment and convert it into motion or mechanical forces. The most prominent examples of these active systems are living organisms, which exhibit striking emergent non-equilibrium behavior such as swarming, lining, vortexes, etc. [7–21]. Synthetic active systems that are able to mimic and reproduce some of the emergent behavior exhibited by living organisms can be used as model systems to study the underlying physical principles which govern their behavior. The activity of the active components can convert energy locally into motion, as in living systems, or induced via an externally applied field or stimuli. Some examples of which include magnetic or electric fields, light-catalyzed

chemical reactions, vibrating granular beds and optical tweezers. Importantly, it is this activity which perpetually drives these systems out-of-equilibrium. However, most biological systems and processes are not composed of purely active components. In biological systems the active or motile components, i.e. cells, are often surrounded by immobile, passive, or even abiotic interfaces. Investigating emergent non-equilibrium behavior in such an artificial model system composed of active and passive components can potentially help distinguish what biological interactions can be attributed to purely physical phenomena and which interactions require presumably physical and biological/biochemical stimuli.

Here, we study a model active matter system that is composed of both passive and active components to study the aggregation of active particles. The active particles rotate in place, henceforth referred to as *spinners*, and are embedded in a dense monolayer of passive particles, as schematically shown in Fig. 1A. In this system, active particles exhibit a long-range attractive interaction [22, 23], which emerges from the non-equilibrium nature of the system and it is mediated by the mechanical properties of the passive medium. We observe that spinners embedded in a dense passive monolayer tend to aggregate forming clusters which grow in time, as schematically shown in Fig. 1. By means of experiments and numerical simulations we demonstrate that this spinner aggregation is driven by the non-equilibrium attractive interaction induced by the mechanical properties of the passive matrix. Moreover, we show that the spinners aggregation process follows a dynamics that resemble a coalescence process. The dynamics of the aggregation process depends on the mechanical properties of the monolayer as well as the activity of the spinners. This type of non-equilibrium attractive interaction opens the

* These two authors contributed equally

† aalexand@mit.edu

door to controlling the state of the system via control of the mechanical properties of the medium, activity of the spinners, and the density of spinners.

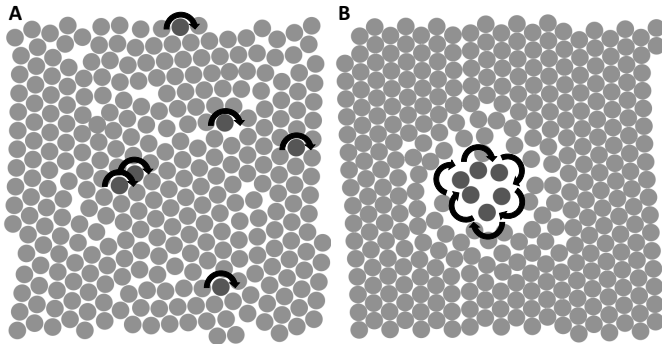


FIG. 1. Schematic representation of the system. A) Co-rotating spinners randomly distributed within a monolayer of passive particles of $\phi_A = 0.8$, which under the action of the magnetic field rotate around the axis perpendicular to the monolayer plane (i.e. z-axis). B) Spinner clusters form due to attraction between active particles.

II. MATERIALS AND METHODS

Our synthetic model system is composed of active spinning particles and passive particles. The spinners are superparamagnetic polymer-based magnetite particles purchased from Bangs Laboratories while the passive particles are composed of polystyrene purchased from Phosphorex; both, active and passive, are $3 \mu\text{m}$ in diameter. We use a concentrated solution of spinners, $\approx 4 \mu\text{g}/\text{mL}$, and passive particles, $\approx 0.8 \text{mg}/\text{mL}$, to study the aggregation and dynamical behavior of the spinners. The spinners are made active by externally applying a magnetic field which rotates around the axis perpendicular to the plane of the monolayer. The solution of spinners and passive particles is inserted into a channel (22mm (L) \times 3mm (W) \times $300\mu\text{m}$ (H)), fabricated using a glass slide, spacer, and cover slip. Once the solution is inserted into the channel it is sealed with epoxy and allowed to sediment for 10 minutes to form a dense monolayer, before being magnetically actuated. The strength of the magnetic field is 5 mT, which is large enough to maintain alignment of the ferromagnetic particles with the rotational frequency of the field. The magnetic field is actuated at an angular frequency, ω , of 5 Hz for approximately 10 minutes. This rotational frequency corresponds to $\text{Re} = 1.25 \times 10^{-6}$. We switch the magnetic field rotational sense every 2 min.

In addition, we carry out numerical simulations of this system. In particular our coarse grained model consists of pseudo-hard sphere particles [24], $N=324$, suspended on a fluid of density $\rho = 1$ and kinetic viscosity $\nu = 1/6$ modeled using the Lattice-Boltzman method. We use the fluctuating Lattice-Boltzmann equation [25]

with $k_B T = 2 \times 10^{-5}$ and the solver D3Q19. We discretized the simulation box in a three dimensional grid of $N_x \times N_y \times N_z = 101 \times 101 \times 20$ bounded in the z direction by no-slip walls and periodic boundary conditions on the x and y directions. We set the grid spacing, Δx and time step, Δt , equal to unity. We apply the bounce-back rule [26] to describe the interaction between the solid particles and the fluid. The particles are treated as real solid objects [27] of diameter $\sigma = 4\Delta x$. The particles settle on the bottom wall of the channel forming a monolayer under the action of a gravitational force, $F_G = 0.005$. The activity is achieved by imposing a constant torque, which in general corresponds to $\text{Re} = 0.72$, unless otherwise noticed.

III. RESULTS AND DISCUSSION

We study the behavior of active rotating particles within monolayers of passive particles. We prepare a dense monolayer composed of passive polystyrene particles, particle area fraction $\phi_A \approx 0.7$, and doped it with a small particle fraction, about 0.5%, of active superparamagnetic particles. Upon actuation of the magnetic field, we observe that spinners aggregate forming nearly circular actively rotating clusters, whose average radius, $\langle R_{\text{cluster}} \rangle$, grows with time, as shown in Fig. 2. These clusters of spinners can be seen growing over time in the experimental snapshots at the top of the figure, where the spinners are the darker spots in the snapshots. This behavior is different than that observed in a system of purely active ferromagnetic and superparamagnetic particles [28–31]. At similar particle area fractions and frequencies in the purely active system the aggregation of particles is dominated by the magnetic dipole-dipole interaction. We observe the formation of small chains or random aggregates [30], which size grows slightly with time. Therefore, the passive monolayer is not only modifying the shape of the aggregates, but also increases the range of the interaction. In fact, in pure equilibrium arguments one would expect the monolayer to strongly retard the aggregation because of the high viscosity of the monolayer.

We carry numerical simulations of this system to study the role of the passive matrix in the spinner aggregation process, and consider whether magnetic dipole-dipole interactions play a mayor role in the spinner aggregation process, particularly at large cluster sizes. Therefore, our coarse grained model neglects the dipole-dipole interactions to isolate the effect of the passive matrix in the spinner aggregation process. In agreement with the experimental results we observe that spinners aggregate forming circular clusters when embedded in dense monolayers of passive particles of $\phi_A = 0.8$. We calculate the time evolution of the area of the active clusters, $A(t)$, for the experimental and simulation trajectories, as shown in Fig. 3. We again observe that the size of the clusters grows with time. Hence, the presence of the passive

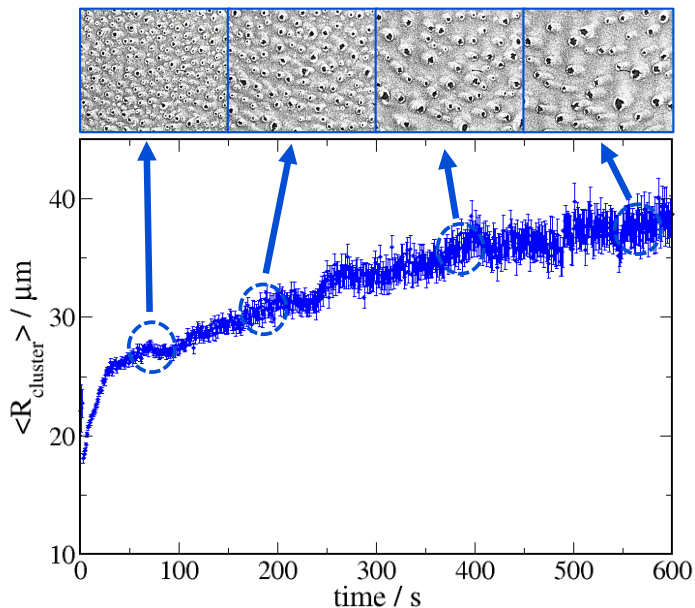


FIG. 2. Average spinner cluster radius, $\langle R_{cluster} \rangle$, as a function of time. The top panel shows several experimental snapshots, which clearly show the average size of the spinner clusters growing over time. The spinners correspond to the darker spots.

monolayer promotes the aggregation of the spinners, even in the absence of magnetic dipole-dipole interactions. In addition, in the simulations we observe that the time evolution of the domain length, $A(t)$, presents important fluctuations due to the absence of dipole-dipole interactions. When two clusters collide, the clusters split in pieces and while the new merged cluster is re-configuring the size of the clusters fluctuates, as shown in Movie 1.

We have recently shown that an attractive interaction emerge between two co-rotating particles, or spinners, if embedded in dense passive monolayers [22, 23]. This emergent attractive interaction and the subsequent non-equilibrium phase separation is thus mediated by the elasticity of the medium and the ability of the spinners to stress that medium. Under the actuation of the rotating magnetic field, the spinners rotate around the axis perpendicular to the substrate generating a rotational fluid flow [32–34]. This causes the surrounding passive particles to rotate due to the momentum transferred through the fluid in which the particles are suspended. In addition, at small but finite Re , the spinner’s rotational motion produces a so-called secondary flow due to the fluid inertia, which pushes away the nearest shell of passive particles, effectively compressing the passive monolayer. Thus, two co-rotating spinners apply compressive and shear stresses on the passive particles located in between the spinners, referred to as the bridge. This produces a stochastic, but steady degradation of the bridge, which allows the spinners to approach resulting in an attractive interaction [22]. Moreover, depending on the mechanical properties of the passive monolayer, this attractive inter-

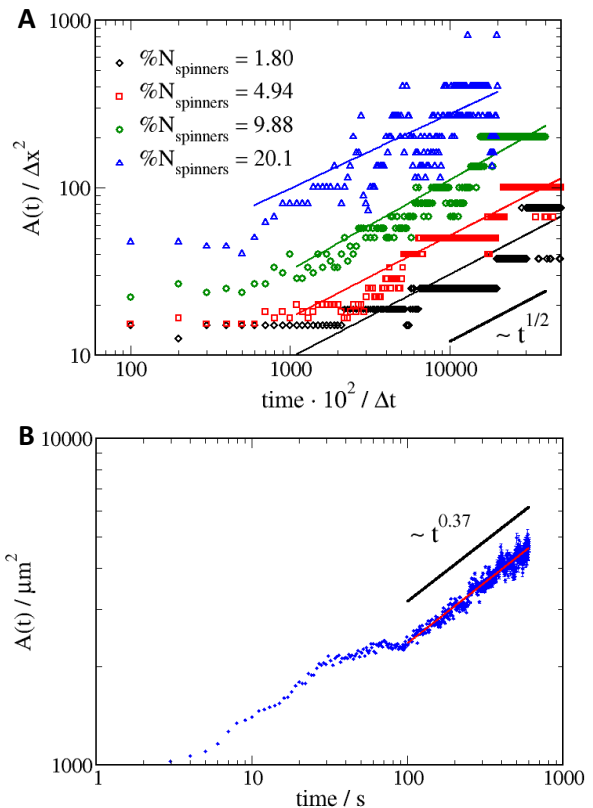


FIG. 3. A) Log - log scale for the spinner cluster size (area), $A(t)$, as a function of time in a passive monolayer of $\phi_A = 0.8$ for four different spinner concentrations: 1.8% (black circles), 4.94% (red squares), 9.88% (green diamonds) and 20.1% (blue triangles) in simulations. B) Log - log scale for the spinner cluster length from experiments as a function of time in a passive monolayer of $\phi_A \approx 0.7$.

action between active rotating particles may be of a very long-range nature [23].

The solid-like character of the passive monolayer induces an attractive interaction between the active particles resulting in the aggregation of the spinners embedded in passive matrixes. However, we do not observe the complete phase separation of the system into passive and active domains for the actuation time period investigated. Instead, spinners aggregate forming clusters which grow with time embedded within the passive matrix. The dynamics of this aggregation process resembles a spinodal decomposition process, in which active clusters coalesce. From the experimental trajectories we compute the time evolution of the number of active clusters, $N(t)$, as shown in Fig. 4A. We observe two different dynamical regimes within the experimental time scale. At short time scales (less than 100s) the clusters exhibit an initial regime of slow cluster growth, or an almost constant number of clusters. This is followed by another regime (after 100s) where the spinner aggregate at a much faster rate. As it can be seen in Fig. 4A, the scaling of the number of

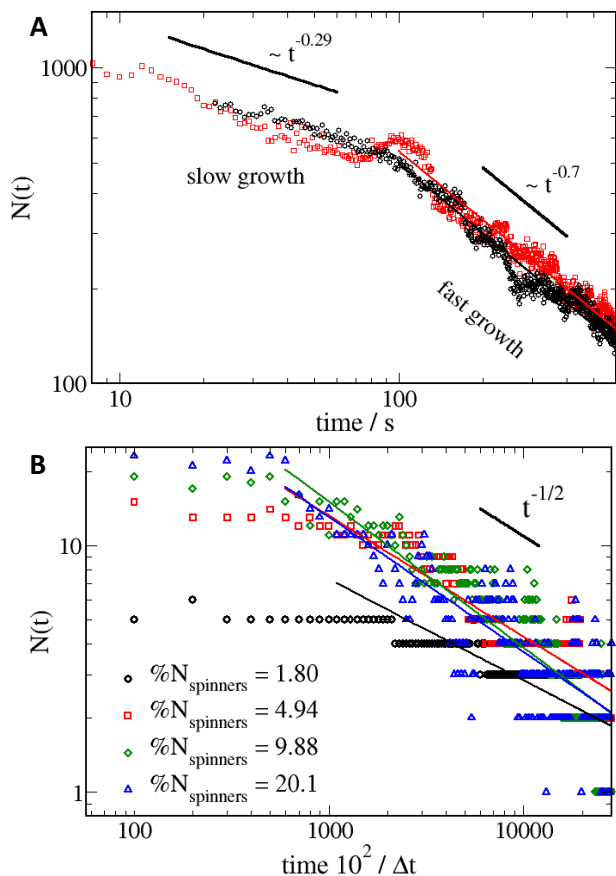


FIG. 4. A) Log - log scale for the number of clusters as a function of time as obtained from the experiments at $\phi_A \approx 0.7$. The two sets of data corresponds to two independent experiments. B) Log - log scale for the number of clusters as a function of time as obtained from the simulation model for four different spinner concentrations at $\phi_A = 0.8$: 1.8% (black circles), 4.94% (red squares), 9.88% (green diamonds) and 20.1% (blue triangles).

clusters with time in this regime is characterized by an exponent of ≈ -0.7 . We also analyze the dynamic scaling of the aggregation of spinners in our simulation model. In this case, we also observe two dynamical regimes: i) An initial slow decrease in the number of clusters (i.e. growth of the cluster sizes), followed by a regime with a dynamic scaling of exponent ≈ -0.5 , as shown in Fig. 4B. Moreover, this dynamic scaling seems independent on the spinner concentration. The $t^{1/2}$ dynamical scaling of the cluster growth has been observed in simulations conducted by Vicsek and several distinct purely active systems, although the origin of this scaling behavior is still unclear [35, 36]. However, we believe that the origin of this scaling behavior is similar to that observed in traditional 2D coarsening [37].

We hypothesize that the difference between the exponents of the dynamic scaling observed in experiments and simulations is due to the magnetic interaction between

clusters of spinners, which increases the strength of the spinner-spinner attraction at short distances. Additionally, this also helps to stabilize spinner clusters. If we also assume a dynamic scaling factor for the slower initial regime in the spinner aggregation process, we obtain for experiments and simulations exponents, $\approx 0.29(2)$ and $\approx 0.04(5)$, respectively. In this first aggregation regime the differences between the experimental and simulation dynamic scaling exponents are much greater than for the second regime. This behavior is in agreement with our hypothesis that the effect of the magnetic dipole-dipole interactions significantly increases the spinner aggregation dynamics. At the beginning of the aggregation process, the active clusters are small and the dipoles of the particles are more easily aligned, which results in higher magnetization of the clusters. In contrast, as the size of the clusters increases, some of the dipoles of the particles are frustrated by the cluster structure, which results in a smaller magnetization of the clusters as their size increases. Therefore, the magnetic interaction is more relevant between smaller clusters than between bigger clusters.

The mechanical properties of the passive media determines the interaction between the spinners and thus, the dynamics of the spinner aggregation. The mechanical properties of the monolayer can be calculated by measuring the mean square displacement (MSD) of the particles in the monolayer in the absence of active particles, specifically the storage and loss modulus, G' and G'' respectively [38, 39]. In simulations, we observe that monolayers of hard-sphere particles at area fractions $\phi_A > 0.7$ respond as viscoelastic materials, behaving as a viscous system at low frequencies and as a solid-like material at high frequencies [22]. However, for $\phi_A < 0.7$ the monolayer behaves as a viscous material over the entire frequency range. To study the effect of the mechanical properties of the monolayer on the dynamics of the spinner aggregation, we investigate, by means of our simulation model, spinners embedded in passive monolayers at different particle area fractions $\phi_A = 0.5, 0.7$, and 0.8 . As it can be seen in Fig. 5, spinners in monolayers of particle area fraction of $\phi_A = 0.8$ and 0.7 follow similar scaling laws. However, at an area fraction of $\phi_A = 0.5$, the spinners do not aggregate within the simulation time scale, as shown by the green diamonds in Fig. 5. The small amount of spinner aggregation observed in Fig. 5 is due to spinners being initially positioned together or close enough so that the removal of a single passive row of particles was required. It should also be noted that for a more dilute concentration of spinners no aggregation is observed in the simulation timescale (data not shown). In addition, at these particle area fractions the monolayer is unable to maintain spinners within a cluster and thus, the number of clusters exhibit large fluctuations. Thus, the presence of a passive monolayer that behaves as a solid-like material induces an attractive interaction between the active rotating particles, which results in aggregation of spinners. Interestingly, the dynamics of the

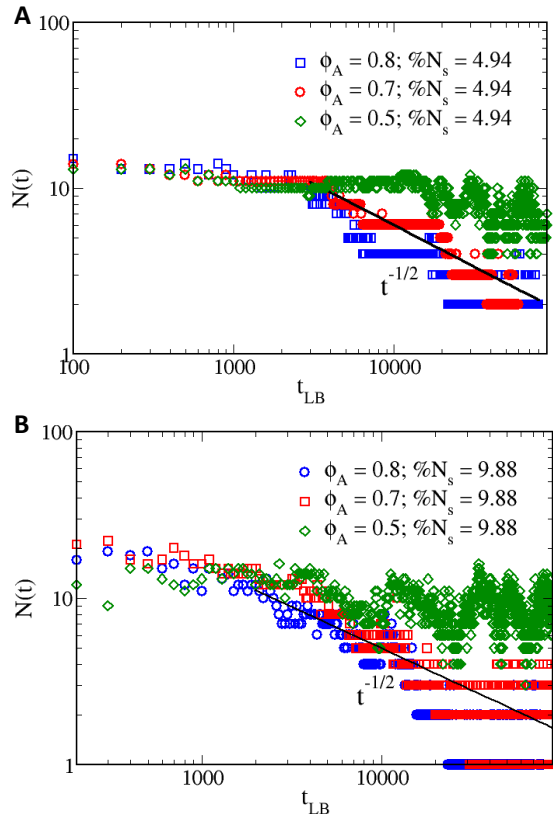


FIG. 5. A) Log - log scale of the time evolution of the number of active clusters at $Re = 0.72$ and a spinner concentration of 4.94% within passive monolayers of $\phi_A = 0.8$ (blue squares), 0.7 (red circles) and 0.5 (green diamonds). B) Log - log scale of the time evolution of the number of active clusters at $Re = 0.72$ and a spinner concentration of 9.88% within passive monolayers of $\phi_A = 0.8$ (blue squares), 0.7 (red circles) and 0.5 (green diamonds).

spinner aggregation seems to be independent of the storage modulus, G' , which is higher for monolayer of $\phi_A = 0.8$ than for monolayer of $\phi_A = 0.7$. This might be due to canceling of two competing effects. On one hand, the effective interaction grows with G' , but on the other hand the motion of the medium is controlled by η , which also grows.

For spinners in a passive monolayer with a packing fraction $\phi_A > 0.7$ the mechanics of the passive monolayer also plays an important role in keeping the cluster of active particles together. We have previously reported that for a system composed of purely active particles the spinners will repel due to the secondary flows generated by the spinners [22, 40]. The spinners within the cluster should then repel, but the passive monolayer exerts a force on the spinners that serves to stabilize the active cluster. This is evident from the stochastic fluctuations shown in the cluster size time evolution, as shown in Fig. 3B and 5, which corresponds to clusters breaking and reforming during the aggregation process. The size

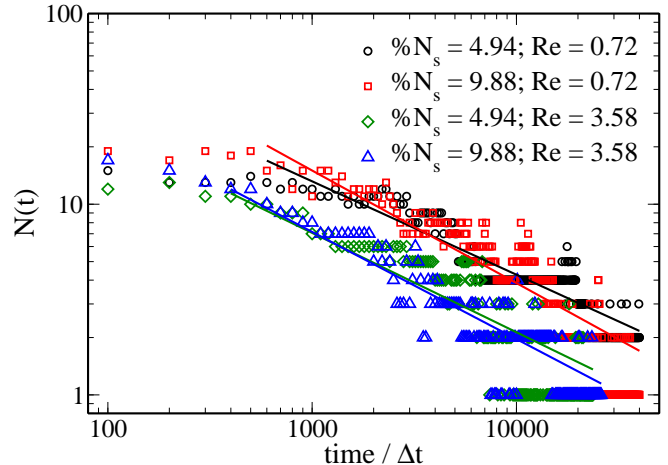


FIG. 6. Aggregation dynamics of spinners within passive monolayers of $\phi_A = 0.8$ at two different rotational frequencies $Re = 0.72$ (black and red symbols) and 3.58 (blue and green symbols) and spinner concentrations 4.94% (circles and diamonds) and 9.88% (squares and triangles).

of the fluctuations increases with the spinners' concentration, due to the bigger size of the clusters.

Aside from the mechanical properties of the monolayer, the other requisite for spinner attraction is the ability to stress the passive monolayer. Therefore, we also explore the effect of the spinners' activity on the aggregation dynamics by applying different rotational frequencies, $Re = 0.1, 0.72$ and 3.58, to spinners embedded in passive matrixes of $\phi_A = 0.8$. In agreement with our previous observations for the spinner-spinner interaction in passive environments [22, 23], we observe there exists a minimum threshold of loading stress, or spinner activity, for the spinner attractive interaction to be important. Spinners rotating at Re smaller than 0.1 do not aggregate. At these activities the stress applied to the passive monolayer is not large enough to promote the occurrence of yielding events, which ultimately results in spinner aggregation [22]. On the contrary, spinners rotating at $Re \geq 0.72$ do aggregate, and the higher the rotational frequency, the faster the evolution of the system, as shown in Fig. 6. Interestingly, the dynamic scaling exponent of the spinner aggregation seems to be independent on the rotational frequency. However, the range of the initial dynamical regime, which probably corresponds to the fastest growing unstable composition mode, shifts towards shorter times. The spinner-spinner attraction in passive matrixes follows activated dynamics [23]. The monolayer region in between the two spinners (i.e. the bridge) needs to be loaded before it yields, which has an associated time scale. This time scale depends on the mechanical properties and configuration of the monolayer. If the stress applied by the spinners overcomes this time

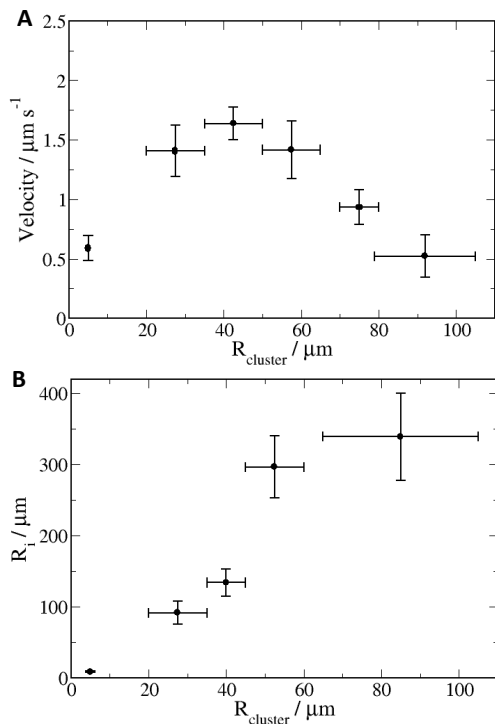


FIG. 7. A) Average approaching velocity of the active clusters as a function of the cluster size (i.e. radius of the cluster). B) Range of the attractive interaction between active clusters as a function of the cluster size. Error bars corresponds to the standard deviation of the trials.

scale, the passive particle mobility increases, resulting in yielding events [22], which leads to the erosion or degradation of the bridge. Therefore, the higher the rotational frequency of the spinners (i.e. Re), the shorter time required to stress the bridge and thus, as the frequency of the spinners increases the faster the growth of the clusters at short time scales. The differences observed between the experiment and simulations on the Re comes from the approximations made in our simulation model. For example, in our simulations the momentum transfer between the spinner and neighboring particles comes exclusively from the fluid, while in the experiment friction and collision between particles may play an important role in transferring momentum.

We further investigate the microscopic details of the spinner aggregation process by tracking the active clusters over time, noting when clusters collide, initial separation distances between clusters which merge, and the velocity at which clusters approach, as shown in Fig. 7. In Fig. 7A, the velocity at which spinner clusters approach as a function of cluster size is presented. We observe that there is a maximum velocity associated with a cluster size of approximately $45\mu\text{m}$. This behavior of cluster velocity as a function of size reveals two competing effects involved in the mobility of the clusters, and therefore their aggregation. The effect which opposes spinner aggregation is the effective drag, which opposes the movement

of the clusters through the monolayer and the drag increases with cluster size. Meanwhile the stress that the spinner cluster can exert on the monolayer increases with the size of the cluster. This increases the frequency of the yielding events resulting in the degradation of the bridge and spinner aggregation. In addition, we observe that the range of the attractive interaction between clusters, R_i , increases with the cluster size, as shown in Fig. 7B. The individual spinner clusters were tracked and as the clusters collide and form bigger clusters the initial distance between colliding clusters was calculated and plotted as a function of the average of the two colliding clusters. As discussed above, the stress exerted on the monolayer increases with the cluster size. Therefore, this increase of the stress on the monolayer produces higher mobility of the passive particles of the monolayer, which results in longer ranged interactions.

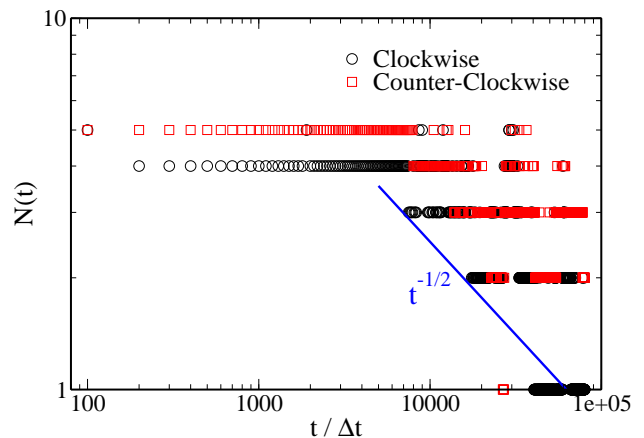


FIG. 8. Aggregation dynamics of spinners rotating clockwise (black circles) at a concentration of 1.54%, and clockwise (red squares) at a concentration of 1.54% within a passive monolayers of $\phi_A = 0.8$.

Finally, we explore the behavior of a ternary mixture in which a passive monolayer is doped with a symmetric mixture of spinners rotating in opposite senses, clockwise and counter-clockwise. In our previous work, we demonstrated that while two co-rotating spinners embedded in a passive matrix experience an attractive interaction, counter-rotating spinners exhibit a repulsive interaction in dense passive environments [22]. We observe that spinners in dense passive monolayers tend form clusters of co-rotating particles and thus, we observe the formation of three different *phases*: i) passive particles, ii) spinners rotating clockwise and iii) spinners rotating counter-clockwise, as shown in Fig. 8. This is the result of the attractive interaction between spinners rotating on the same direction, and the repulsive interaction between spinners rotating on opposite directions.

IV. CONCLUSIONS

We studied the aggregation of active rotating particles embedded in passive monolayer. We demonstrate that the non-equilibrium attractive interaction between spinners within dense passive matrixes [22, 23] results in their aggregation. This aggregation resembles a 2D coarsening [37], which has also been described for other pure active systems [35, 36]. Although, the system size we can reach does not allow us to unambiguously determine the dynamic scaling exponent of the spinner aggregation process. We explore the effect of the particle area fraction of the monolayer, spinner concentration and spinner activity on the aggregation behavior. We observe that the monolayer must behaves as a solid, $\phi_A > 0.7$, in order to observe spinner aggregation. In addition, for the spinners to stress the monolayer and thus, produces yielding events that result into the attraction of spinners,

there is a minimum activity threshold, $Re > 0.1$ in simulations. Interestingly, the aggregation dynamics seems to be independent of the spinner concentration. We also study the microscopic details of the cluster aggregation. We observe that spinner clusters move faster as the size increases up to reach a velocity maximum at around $R_{cluster} = 45 \mu\text{m}$. Finally, we show that a ternary mixture of passive particles, co-rotating and counter-rotating spinners results into the formation of cluster of spinner with the same sense of rotation. This is due to the fact that co-rotating spinners with in a dense passive monolayer attract each other while counter-rotating spinner repel.

V. ACKNOWLEDGMENTS

This work was supported by Department of Energy BES award #ER46919 (theoretical and simulation work) and the Chang Family (experimental work).

-
- [1] J. D. Gunton, M. San Miguel, and P. Sahni, *Phase Transition and Critical Phenomena*, Vol. 8 (Academic, London, 1983).
 - [2] J. Palacci, S. Sacanna, A. P. Steinberg, D. J. Pine, and P. M. Chaikin, *Science* **339**, 936 (2013).
 - [3] L. Corté, P. M. Chaikin, J. P. Gollub, and D. J. Pine, *Nature Physics* **4**, 420 (2008).
 - [4] T. Ishikawa and T. J. Pedley, *Phys. Rev. Lett.* **100**, 088103 (2008).
 - [5] A. P. Berke, L. Turner, H. C. Berg, and E. Lauga, *Phys. Rev. Lett.* **101**, 038102 (2008).
 - [6] K. Drescher, K. C. Leptos, I. Tuval, T. Ishikawa, T. J. Pedley, and R. E. Goldstein, *Phys. Rev. Lett.* **102**, 168101 (2009).
 - [7] J. Buhl, D. J. T. Sumpter, I. D. Couzin, J. J. Hale, E. Despland, E. R. Miller, and S. J. Simpson, *Science* **312**, 1402 (2006).
 - [8] N. C. Darnton, L. Turner, S. Rojevsky, and H. C. Berg, *Biophysical Journal* **98**, 2082 (2010).
 - [9] A. Ordemann, G. Balazsi, and F. Moss, *Physica A: Statistical Mechanics and Its Applications* **325**, 260 (2003).
 - [10] Y. Wu, A. D. Kaiser, Y. Jiang, and M. S. Alber, *PNAS*, pnas.0811662106 (2009).
 - [11] H. P. Zhang, A. Be'er, E.-L. Florin, and H. L. Swinney, *PNAS* **107**, 13626 (2010).
 - [12] S.-N. Lin, W.-C. Lo, and C.-J. Lo, *Soft Matter* **10**, 760 (2014).
 - [13] J. Toner and Y. Tu, *Physical Review E* **58**, 4828 (1998).
 - [14] M. Ballerini, N. Cabibbo, R. Candelier, A. Cavagna, E. Cisbani, I. Giardina, V. Lecomte, A. Orlandi, G. Parisi, A. Procaccini, M. Viale, and V. Zdravkovic, *PNAS* **105**, 1232 (2008).
 - [15] A. Cavagna, A. Cimorelli, I. Giardina, G. Parisi, R. Santagati, F. Stefanini, and M. Viale, *PNAS* **107**, 11865 (2010).
 - [16] J. L. Silverberg, M. Bierbaum, J. P. Sethna, and I. Cohen, *Physical Review Letters* **110**, 228701 (2013).
 - [17] B. Szabó, G. J. Szöllösi, B. Gönci, Z. Jurányi, D. Selmecezi, and T. Vicsek, *Physical Review E* **74**, 061908 (2006).
 - [18] D. F. Hinz, A. Panchenko, T.-Y. Kim, and E. Fried, *Soft Matter* **10**, 9082 (2014).
 - [19] H. Wioland, F. G. Woodhouse, J. Dunkel, J. O. Kessler, and R. E. Goldstein, *Physical Review Letters* **110**, 268102 (2013).
 - [20] T. Sanchez, D. T. N. Chen, S. J. DeCamp, M. Heymann, and Z. Dogic, *Nature* **491**, 431 (2012).
 - [21] J.-F. Joanny and S. Ramaswamy, *Nature* **467**, 33 (2010).
 - [22] J. L. Aragonés, J. P. Steimel, and A. Alexander-Katz, *Nature Communications* **7**, 11325 (2016).
 - [23] J. P. Steimel, J. L. Aragonés, H. Hu, N. Qureshi, and A. Alexander-Katz, *Proceedings of the National Academy of Sciences* **113**, 4652 (2016).
 - [24] J. Jover, A. J. Haslam, A. Galindo, G. Jackson, and E. A. Muller, *Journal of Chemical Physics* **137**, 144505 (2012).
 - [25] B. Dünweg and A. Ladd, *Adv Polym Sci*, 1 (2008).
 - [26] A. J. C. Ladd, *J. Fluid. Mech.* **271**, 285 (1994).
 - [27] E.-J. Ding and C. K. Aidun, *Journal of Statistical Physics* **112**, 685 (2003).
 - [28] M. Kalontarov, M. T. Tolley, H. Lipson, and D. Erickson, *Microfluidics and Nanofluidics* **9**, 551 (2010).
 - [29] J. H. E. Promislow, A. P. Gast, and M. Fermigier, *The Journal of Chemical Physics* **102**, 5492 (1995).
 - [30] J. Richardi and J.-J. Weis, *The Journal of Chemical Physics* **135**, 124502 (2011).
 - [31] Y. Gao, M. A. Hulsen, T. G. Kang, and J. M. J. den Toonder, *Physical review. E, Statistical, nonlinear, and soft matter physics* **86**, 041503 (2012).
 - [32] E. Climent, K. Yeo, M. R. Maxey, and G. E. Karniadakis, *Journal of Fluids Engineering* **129**, 379 (2007).
 - [33] B. A. Grzybowski, X. Jiang, H. Stone, and G. M. Whitesides, *Physical review. E, Statistical, nonlinear, and soft matter physics* **64**, 011603 (2001).

- [34] B. Grzybowski, H. Stone, and G. Whitesides, *Nature* **405**, 1033 (2000).
- [35] S. Dey, D. Das, and R. Rajesh, *Phys. Rev. Lett.* **108**, 238001 (2012).
- [36] G. S. Redner, M. F. Hagan, and A. Baskaran, *Physical Review Letters* **110**, 055701 (2013).
- [37] K. Binder and D. Stauffer, *Physical Review Letters* **33**, 1006 (1974).
- [38] T. Mason and D. Weitz, *Physical Review Letters* **74**, 1250 (1995).
- [39] T. G. Mason, *Rheologica acta* **39**, 371 (2000).
- [40] Y. Goto and H. Tanaka, *Nature Communications* **6**, 1 (2016).